Gradient-Based Excitation Filter for Molecular Ground-State Simulation

Runhong He[1], Qiaozhen Chai[1], Xin Hong[1], Ji Guan[1], Guolong Cui[2], Shengbin Wang[3], Shenggang Ying[1*]

1. Key Laboratory of System Software (Chinese Academy of Sciences) and State Key Laboratory of Computer Science, Institute of Software, Chinese Academy of Sciences, Beijing 100190, China

2. Arclight Quantum Co., LTD. Chinese Academy of Sciences, Beijing 101408, China

3. China Telecom Quantum Information Technology Group Co., LTD, Hefei 233000, China

E-mail: *yingsg@ios.ac.cn

July 2025

Abstract. Molecular ground-state simulation is one of the most promising fields for demonstrating practical quantum advantage on near-term quantum computers. However, the Variational Quantum Eigensolver (VQE), a leading algorithm for this task, still faces significant challenges due to excessive circuit depth. This paper introduces a method to efficiently simplify the Unitary Coupled-Cluster with Single and Double Excitations (UCCSD) ansatz on classical computers. We propose to estimate the correlation energy contributions of excitations using their gradients at Hartree-Fock state, supported by a theoretical proof. For molecular systems with K orbitals, these gradients can be obtained with complexity only $O(K^8)$, which can be efficiently implemented on classical computers, especially in parallel. By sorting and truncating the excitations based on these gradients, the simplified ansatz can be obtained immediately, avoiding the challenging task of optimizing ansatz structure on a quantum computer. Furthermore, we introduce a strategy to indirectly identify critical excitations through spin-adapted constraints, reducing gradient computations by 60%. Numerical experiments on prototype molecular systems (H_4, HF, H_2O, BeH_2 and NH_3) demonstrate that our approach achieves up to 46% parameter decrease, 60% circuit depth reduction and 678× runtime speedup compared to state-of-the-art benchmarks (ADAPT-VQE and SymUCCSD), enabling significantly more compact quantum circuits with enhanced near-term feasibility.

Keywords: Quantum Computational Chemistry, Variational Quantum Eigensolver, UCCSD Ansatz

1. INTRODUCTION

The chemical properties of matter are fundamentally determined by molecular energy levels [1]. This relationship is particularly evident in chemical kinetics, where accurate prediction of reaction rates requires precise knowledge of ground-state energies [2]. Within classical computational frameworks, molecular energies can be exactly determined through the Full Configuration Interaction (FCI) method [3]. However, the FCI method's computational cost scales exponentially with system size, making it feasible only for small molecular systems [4]. For larger molecular systems, approximations have to be introduced to balance computational cost and accuracy. A prominent example is the Coupled-Cluster Singles and Doubles (CCSD) method, which truncates the cluster operator at single and double excitations, significantly reducing computational complexity. As low energy excitations dominate the ground state in many systems, this truncation can still yield good approximations to the ground-state energy [1, 4].

Quantum algorithms that leverage the properties of quantum superposition and entanglement can achieve significant speedup over classical algorithms in solving certain important problems [5]. The first quantum algorithm capable of solving Hamiltonian eigenvalue problems is the Quantum Phase Estimation (QPE) algorithm [6]. Compared to classical algorithms, QPE can provide exponential speedup. However, the quantum hardware requirements for QPE – including error correction mechanisms and long coherence times – currently exceed the capabilities of near-term Noisy Intermediate-Scale Quantum (NISQ) devices [7]. Recently, the Variational Quantum Eigensolver (VQE) algorithm [8, 9, 10, 11], which adopts a quantum-classical hybrid architecture, has attracted wide-spread attention. In VQE, the second-quantized Hamiltonian can be transformed into Pauli strings through established encodings such as Jordan-Wigner [12] or Bravyi-Kitaev [13], thereby enabling the expectation value of the trial state with respect to the Hamiltonian to serve as the eigenvalue. During practical execution of VQE, the quantum processor runs a parameterized quantum circuit (ansatz circuit) to generate trial states, while the classical computer calculates the loss function and gradients based on measurement outcomes. These results are then used to update the parameters in the ansatz circuit to obtain improved solutions. Compared to the QPE algorithm, VQE features shallower circuit depths and holds promise for practical implementation in the NISQ era.

The design of the ansatz circuit lies at the heart of the VQE. In contrast to the hardware-efficient ansatz [14] – which, while readily implementable, is plagued by the barren plateau problem [15] – the Unitary Coupled-Cluster with Single and Double Excitations (UCCSD) method [1] has attracted extensive attention and in-depth investigation, owing to its clear physical interpretation and robust convergence properties. The UCCSD ansatz requires transformation of fermionic excitations into parameterized quantum circuits through two primary approaches. (1) Conventional Pauli-based implementation [16, 17]: excitations are first mapped to Pauli strings

via encodings [12, 13], which are then synthesized into quantum circuits through exponentiation techniques [5]. (2) Emerging direct construction methods [18, 19, 20]: these circumvent the Pauli decomposition by directly implementing excitations via combining C^nR_y gate and basis transformation operations, thereby significantly improving computational efficiency.

The implementation cost of the UCCSD ansatz is dominated by double excitations, whose number scales with system size as $O(K^4)$ for K molecular orbitals. This scaling inevitably generates quantum circuit depths surpassing the error tolerance limits of NISQ hardware, precluding simulations of industrially meaningful molecules. It is crucial to emphasize that not all excitations in the UCCSD ansatz contribute equally – a substantial fraction have only negligible effects on ground-state energy. Therefore, accurately identifying and filtering out redundant excitations in the UCCSD ansatz is essential for reducing quantum circuit depth and advancing the practical application of VQE algorithms.

To address this problem, Ref. [21] proposed a compression method named "SymUCCSD" based on molecular point group symmetry. SymUCCSD systematically eliminates symmetry-violating excitations, but suffers from two limitations: (1) It's efficacy strongly depends on molecular symmetry – it achieves substantial ansatz compression for highly symmetric systems but shows limited improvement for low-symmetry molecules. (2) It retains symmetry-compliant yet energetically negligible ("non-important") excitation operators, leaving residual redundancies in the simplified ansatz.

The ADAPT-VQE algorithm [22] provides an innovative approach to excitation selection. It utilizes an "Excitation Pool" containing all UCCSD excitations and constructs a compact quantum circuit from identity by dynamically adding only the most energetically significant excitations (selected based on gradient magnitudes) at each iteration. Compared to fixed ansatz such as the standard UCCSD and SymUCCSD, ADAPT-VQE achieves chemical accuracy with significantly fewer parameters while maintaining comparable precision. Furthermore, this method demonstrates remarkable generality, being applicable to ground-state energy calculations across diverse molecular systems. These advantages have propelled the ADAPT-VQE to rapid widespread adoption since its inception, establishing it as a leading approach in the field [17, 20, 23, 24, 25, 26, 27]. However, the ADAPT-VQE suffer from non-negligible inefficiencies that fundamentally limit their applicability to larger molecular systems: each iteration requires (1) evaluating the gradients of all excitations in the Excitation Pool in current trial state, and (2) re-optimizing all parameters in the expanded ansatz after adding a new excitation. Specifically, for an UCCSD ansatz containing N excitations (of which M are energetically significant), the ADAPT-VQE algorithm requires $O(M)$ VQE optimization procedures, accumulatively optimizes $O(M^2)$ parameters in total, and performs $O(N \times M)$ excitation gradient evaluations during the selection process. Here, a "VQE optimization procedure" refers to the end-to-end computational process encompassing: (1) ansatz parameter initialization, (2) iterative parameter updates via

hybrid quantum-classical feedback, and (3) convergence verification against predefined thresholds.

In this work, we establish a theoretical connection between the excitations' gradients at Hartree-Fock state and their correlation energy contributions, thereby developing an efficient excitation selection algorithm. We term this algorithm GBEF (Gradient-Based Excitation Filter). After compressing both the system Hamiltonian and Hartree-Fock state into the excitation's subspace, each gradient can be computed with complexity comparable to 16×16 matrix multiplication. This contrasts with ADAPT-VQE, which approximates gradients for quantum hardware-prepared ansatz states through costly measurements. GBEF leverages these gradients to systematically sort and truncate redundant excitations, achieving significant efficiency gains over iterative ADAPT-VQE. For a K-orbital molecular system, GBEF achieves $O(K^8)$ computational complexity, allowing efficient parallel implementation on classical computers. Moreover, our method requires no prior knowledge of molecular symmetry, making it applicable to a wider range of molecular systems than SymUCCSD. Finally, we introduce a parameter-based strategy for indirectly selecting critical excitations, leveraging spin-adaption constraints to reduce the number of gradient calculations by about 60%.

2. Methods

2.1. Specification of the adopted notations

To construct the method, we introduce the following definitions and notation. First, the occupied molecular orbitals are indexed with subscripts a and b, while virtual orbitals are indexed with r and s.

In UCCSD, the trail state $|\Psi(\vec{\theta})\rangle$ is prepared from the Hatree-Fock state $|HF\rangle$ by an unitary evolution operator (ansatz) $\mathrm{e}^{T(\vec{\theta})}$ involving single and double excitations [1]:

$$|\Psi(\vec{\theta})\rangle = \mathrm{e}^{T(\vec{\theta})}|HF\rangle, \tag{1}$$

with the exponent

$$T(\vec{\theta}) = \sum_{r,a} \theta_a^r A_a^r + \sum_{r>s,a>b} \theta_{ab}^{rs} A_{ab}^{rs}. \tag{2}$$

The single and double excitations are defined as

$$A_a^r = \hat{a}_r^\dagger \hat{a}_a - \hat{a}_a^\dagger \hat{a}_r, \quad A_{ab}^{rs} = \hat{a}_r^\dagger \hat{a}_s^\dagger \hat{a}_a \hat{a}_b - \hat{a}_a^\dagger \hat{a}_b^\dagger \hat{a}_r \hat{a}_s, \tag{3}$$

where operators $\hat{a}_i^\dagger$ (creation) and $\hat{a}_i$ (annihilation) obey fermionic anti-commutation rules:

$$\{\hat{a}_i, \hat{a}_j^\dagger\} = \delta_{i,j}, \quad \{\hat{a}_i, \hat{a}_j\} = \{\hat{a}_i^\dagger, \hat{a}_j^\dagger\} = 0. \tag{4}$$

Under first-order Trotter-Suzuki approximation [28], the evolution operator can be decomposed as:

$$\mathrm{e}^{T(\vec{\theta})} \approx \prod_k \mathrm{e}^{\theta_k A_k}, \tag{5}$$

where each A_k represents either a single excitation A_a^r, or a double excitation A_{ab}^{rs}. The quantum circuit implementation of excitations has been extensively investigated in the literature, featuring various overheads that include: encodings [12, 29, 13], qubit excitations [16] and efficient circuit designs [18, 20, 19]. This work focuses only on simplifying the UCCSD ansatz by reducing the number of excitations, without considering their implementation details.

In conventional VQE implementations, excitation parameters are typically optimized as independent variables. This approach, while flexible, does not inherently preserve the spin symmetry of the resulting wavefunction, as the final trial state may not remain an eigenstate of the $\hat{S}^2$ operator. For systems where the exact ground state is expected to maintain definite spin symmetry (particularly in closed-shell configurations), we can impose the spin-adaptation constraints on the excitations. These constraints enforce commutativity between the excitations and $\hat{S}^2$, thereby guaranteeing spin-preserving solutions while simultaneously reducing the number of free variational parameters. By reinterpreting the subscripts in Eq. (2) to denote spatial (rather than spin) orbitals and explicitly indicating spin flavors (α/β), we can derive explicit spin-adaptation constraints for closed-shell configurations [30]:

$$\theta_{a_\alpha}^{r_\alpha} = \theta_{a_\beta}^{r_\beta}, \tag{6}$$

$$\theta_{a_\alpha b_\alpha}^{r_\alpha s_\alpha} = \theta_{a_\beta b_\beta}^{r_\beta s_\beta} = \theta_{a_\alpha b_\beta}^{r_\alpha s_\beta} + \theta_{a_\alpha b_\beta}^{r_\beta s_\alpha}, \tag{7}$$

$$\theta_{a_\alpha b_\beta}^{r_\alpha s_\beta} = \theta_{a_\beta b_\alpha}^{r_\beta s_\alpha} \quad \& \quad \theta_{a_\alpha b_\beta}^{r_\beta s_\alpha} = \theta_{a_\beta b_\alpha}^{r_\alpha s_\beta}, \tag{8}$$

$$\theta_{a_\alpha b_\beta}^{r_\alpha r_\beta} + \theta_{a_\beta b_\alpha}^{r_\alpha r_\beta} = \theta_{a_\alpha a_\beta}^{r_\alpha s_\beta} + \theta_{a_\alpha a_\beta}^{r_\beta s_\alpha} = 0. \tag{9}$$

While the spin-adaptation constraints do not reduce the number of excitations in the ansatz, they significantly decrease the number of free parameters to be optimized, thereby reducing the measurement cost in VQE optimization. Compared to conventional approaches treating each excitation individually, systematic application of spin-adaptation constraints typically enables a $\sim 60\%$ reduction in parameter counts while preserving wavefunction accuracy.

In the framework of VQE, the ground-state engergy is obtained by minizing the expectation value of the Hamitonian with respect to the ansatz parameters:

$$E = \min_{\vec{\theta}} \langle \Psi(\vec{\theta}) | \mathscr{H} | \Psi(\vec{\theta}) \rangle. \tag{10}$$

Within the Born-Oppenheimer approximation, the second-quantized electronic Hamiltonian of a molecule in atomic units takes the form [1]

$$\mathscr{H} = \sum_{a,r} h_a^r \hat{a}_r^\dagger \hat{a}_a + \frac{1}{2} \sum_{a,b,r,s} h_{ab}^{rs} \hat{a}_r^\dagger \hat{a}_s^\dagger \hat{a}_a \hat{a}_b, \tag{11}$$

with one- and two-electron integrals in a spin-orbital basis [31]

$$h_a^r = \int d\mathbf{x} \phi_r^*(\mathbf{x}) \left(-\frac{\nabla^2}{2} - \sum_I \frac{Z_I}{|\mathbf{r} - \mathbf{R}_I|} \right) \phi_a(\mathbf{x}), \tag{12}$$

$$h_{ab}^{rs} = \int \mathrm{d}\mathbf{x}_1 \mathrm{d}\mathbf{x}_2 \frac{\phi_r^*(\mathbf{x}_1)\phi_s^*(\mathbf{x}_2)\phi_a^*(\mathbf{x}_2)\phi_b^*(\mathbf{x}_1)}{|\mathbf{r}_1 - \mathbf{r}_2|}. \tag{13}$$

where Z_I, $\mathbf{R}_I$ and $\mathbf{r}_1$ denote the atomic number and position of the I-th nucleus and position of the i-th electron, respectively. These integrals can be efficiently computed within specified basis sets, such as the STO-3G basis set. When calculating the expectation value of the Hamiltonian (11), it is necessary to transform it from the second-quantized form to a Pauli string representation through encodings [12].

2.2. Gradient-Based Excitation Filter Algorithm

To simplify the UCCSD ansatz, we establish the following theorem (proof is provided in Appendix 5).

Theorem 1. *If the Hartree-Fock state $|HF\rangle$ is a good approximation to the exact ground state wave-function $|\Phi_0\rangle$, an excitation's contribution to the correlation energy is related to the gradient of the system energy involved only this excitation at the $|HF\rangle$ with respect to the coefficient $\theta = 0$.*

This theorem points to an efficient path to filter out redundant excitations in the UCCSD ansatz. Since double (single) excitations act on only 4 (2) qubits, we can easily compute excitations' gradients by compressing the full system Hamiltonian and Hartree-Fock state into this small subspace. This enables efficient estimation of each excitation's relative contribution to the correction energy through the Thm. 1.

The overview of our GBEF algorithm and its integration with the standard VQE workflow is drawn schematically in Fig. 1 and is as follows:

(1) According to the molecular information, compute one- and two-electron integrals in Eq. (11) at a chosen basis set, and apply fermion-to-qubit encoding (e.g., the Jordan-Wigner encoding [12]) to obtain the full Hamiltonian in Pauli representation. Construct the Hatree-Fock state $|HF\rangle$ and the UCCSD ansatz.

(2) Randomly assign to each parameter θ_k in the UCCSD ansatz an excitation A_k that is only associated with θ_k. These parameter-excitation pairs collectively form a set denoted as $\{(\theta_k, A_k)\}$.

(3) For each element in $\{(\theta_k, A_k)\}$, project: the excitation itself ($A_k \to \widetilde{A_k}$), the full Hamitonian ($\mathscr{H} \to \widetilde{\mathscr{H}_k}$), the Hartree-Fock state ($|HF\rangle \to |\widetilde{HF}\rangle_k$) onto the corresponding 4-qubit (2-qubit) subspace for double (single) excitation, thereby forming a new set denoted as $\{(\theta_k, \widetilde{A_k}, \widetilde{\mathscr{H}_k}, |\widetilde{HF}\rangle_k)\}$.

(4) For each element in $\{(\theta_k, \widetilde{A_k}, \widetilde{\mathscr{H}_k}, |\widetilde{HF}\rangle_k)\}$, compute system energy's gradient with respect to $\theta_k = 0$ at $|\widetilde{HF}\rangle_k$ via

$$\nabla_k E_k := \frac{\mathrm{d}E_k}{\mathrm{d}\theta_k}\Big|_{\theta_k=0} = {}_k\langle\widetilde{HF}|[\widetilde{\mathscr{H}_k}, \widetilde{A_k}]|\widetilde{HF}\rangle_k, \tag{14}$$

where $E_k := {}_k\langle\widetilde{HF}|\mathrm{e}^{-\theta_k\widetilde{A_k}}\widetilde{\mathscr{H}_k}\mathrm{e}^{\theta_k\widetilde{A_k}}|\widetilde{HF}\rangle_k$. This step can be easily calculated with computational complexity comparable to 16×16 (4×4) matrix multiplication for double (single) excitations.

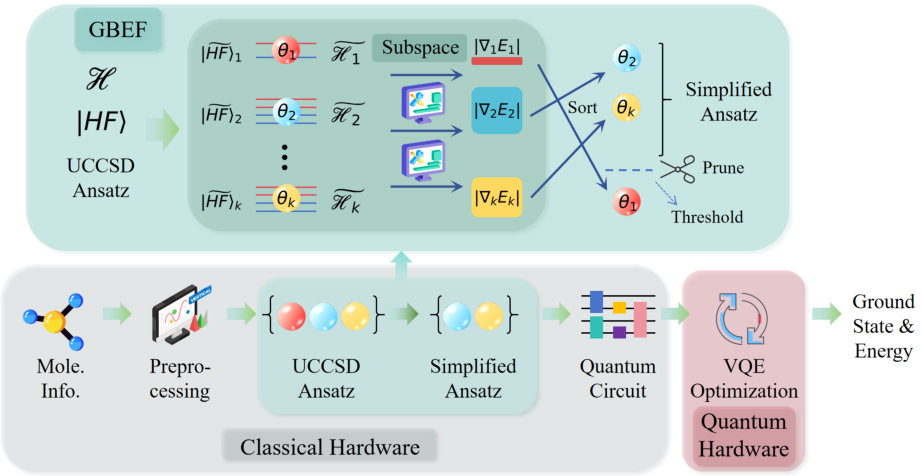

Figure 1: Schematic depiction of the GBEF algorithm and its integration with the standard VQE workflow.

(5) List and sort all parameters θ_k in descending order based on their corresponding absolute gradient values $|\nabla_k E_k|$.

(6) Prune the parameter sequence according to a certain strategy, yielding an optimized parameter subset $\{\theta_k\}_{\text{opt}}$.

(7) Collect all excitations in UCCSD that associated with parameters in $\{\theta_k\}_{\text{opt}}$, and combine them to form the simplified ansatz, thereby generating the corresponding quantum circuit.

(8) Perform standard VQE optimization procedure using the constructed quantum circuit to determine the molecular ground-state energy.

As described above and illustrated in Fig. 1, the distinctive workflow of our GBEF algorithm for UCCSD ansatz simplification includes operates from Step 2 to Step 7. Specifically, in Steps 2 and 7, we propose an excitation-grouping strategy based on free parameters that fully exploits spin-adaptation constraints to reduce gradient computations by about 60%. In Steps 3-4, we compress both the full Hamiltonian and Hartree-Fock state into the subspace of excitations, enabling efficient classical computation of parameter gradients. Since the gradient computation for each excitation incurs fixed costs, the dominant computational expense in GBEF stems from the Hamiltonian compression. For a system with K molecular orbitals, where both the number of excitations and terms in Hamiltonian scale as $O(K^4)$, the overall complexity of these two steps is $O(K^8)$ — a process can be efficiently handled by classical computers, especially in parallel. In Steps 5-6, we sort and truncate parameters according to the absolute values of their gradients, thereby identifying the unessential parameters to filter out. The truncation threshold can be adjusted to balance accuracy and efficiency. Steps 1 and 8 ensures end-to-end compatibility with the existing VQE workflow.

Table 1: Qubit requirements, bond types and bond length ranges for quantum simulations of the investigated molecules. 21 equally spaced points are sampled across the range of bond distances to draw a statistical conclusion.

Molecule	Qubit Count in VQE	Bond Type	Equilibrium Bond Length (Å)	Bond Length Range (Å)
H_4	8	H-H	0.89	$[0.1, 1.1]$
HF	12	F-H	0.99	$[0.1, 1.1]$
H_2O	14	O-H	1.02	$[0.1, 1.2]$
BeH_2	14	Be-H	1.32	$[0.1, 1.4]$
NH_3	16	N-H	1.05	$[0.1, 1.1]$

3. Results

In this section, we investigate the performance of our GBEF algorithm in finding equilibrium geometries for 5 typical molecules: H_4, HF, H_2O, BeH_2, and NH_3. Tab. 1 comprehensively characterizes the studied molecular systems, including bond types, equilibrium bond lengths and scanned bond length ranges for geometry optimization. The number of qubits required for VQE implementation serves as a metric for molecular system size.

To implement the numerical experiments, we compute electronic integrals, FCI ground-state energy, and construct the system Hamiltonian using the OpenFermion package [32] in the STO-3G basis set, simulate quantum circuits and perform gradient calculations in VQE procedure via the MindSpore Quantum platform [33], and employ the gradient-based Broyden–Fletcher–Goldfarb–Shannon (BFGS) algorithm [34] for parameter optimization. The algorithms (GBEF and ADAPT-VQE) are run on an 16-core 2.10 GHz CPU with 120 GB memory and an RTX 4090 (24GB) GPU.

Tab. 2 compares the parameter reduction performance of our GBEF algorithm with

Table 2: Parameter reduction performance benchmarks comparing GBEF (with ablation studies) against standard UCCSD, ADAPT-VQE, and SymUCCSD: parameter counts, reduction ratios, and GBEF's truncation thresholds.

Molecule	Number of Parameters							Reduction**		Threshold	
	UCCSD	ADAPT-			Sym-UCCSD	GBEF	Ablation	GBEF	Ablation	abs	mag
		ϵ_1*	ϵ_2	ϵ_3							
H_4	14	5.33(52.38%)	6.86	7.81	8	5.52	5.33	19.53%	22.3%	0.05	0.50
HF	20	2.09(90.48%)	6.81	10.05	11	4.38	2.14	35.68%	68.58%	0.06	0.45
H_2O	65	5.24(19.05%)	18.62	24.52	26	10.05	8.67	46.03%	53.44%	0.05	0.27
BeH_2	90	7.33(33.33%)	18.90	22.71	23	10.67	8.71	43.54%	53.92%	0.04	0.30
NH_3	135	6.67(0%)	57.95	85.19	75	44.52	32.71	23.18%	43.36%	0.017	0.40

* The ADAPT-ϵ_1 algorithm's overly relaxed convergence threshold led to out-of-tolerance VQE errors (parentheses show the percentage of cases achieving chemical accuracy). In contrast, all other methods achieve chemical precision throughout.

** These percentages are benchmarked against ADAPT-ϵ_2's results, which guarantee chemical accuracy throughout and represent the lowest parameter count among existing approaches.

UCCSD, ADAPT-VQE, and SymUCCSD benchmarks, including ablation studies and the pruning threshold used in GBEF. In the ADAPT-VQE algorithms, the convergence threshold $\epsilon_m = 10^{-m}$ specifies the termination criterion for the iterative procedure [22]. Generally, a smaller value of m in ADAPT-VQE generates more compact ansatze with fewer parameters, but risks introducing errors that may violate the chemical accuracy threshold (defined as a 1.6 mHa deviation from FCI results) in the final VQE solutions. The GBEF algorithm employs a dual-threshold parameter truncation strategy in Step 6 that combines both absolute and relative criteria. First, parameters with gradients below the absolute threshold "abs" are systematically discarded to eliminate physically insignificant contributions. Subsequently, the remaining parameters undergo relative importance evaluation, where the parameter list is truncated at the point where sequential gradients exhibit a 10^{mag}-fold decrease in their norms, thereby retaining only the most dominant parameters while maintaining computational efficiency. The thresholds abs and mag can be adjusted according to the gradient list to achieve an optimal balance between circuit depth and solution accuracy. This hierarchical approach ensures robust parameter selection by considering both the absolute physical significance and relative quantitative importance of each term. In the GBEF ablation study, we progressively eliminate parameters with the smallest gradients from the pre-sorted list (obtained in Step 5) until attaining the minimal parameter set that preserves chemical accuracy in VQE results, representing the practical performance limit of the GBEF.

As evidenced in Tab. 2, our GBEF algorithm and its ablation achieve the best performance, reducing parameter counts by 20-46% and 22-69% respectively compared to the ADAPT-ϵ_2 algorithm, while maintaining chemical accuracy in all VQE results. The Ablation results also reveal substantial optimization potential in our GBEF algorithm, particularly through developing more advanced truncation protocols for Step 6.

Table 3: Comparison of final Ansatz circuit depths between the GBEF and ADAPT-VQE algorithms. All excitations are implemented using the Jordan-Wigner encoding [12].

Molecule	ADAPT-			GBEF	Ablation	Reduction*	
	ϵ_1	ϵ_2	ϵ_3			GBEF	Ablation
H_4	451.14	641.43	692.90	544.81	544.81	15.06%	15.06%
HF	148.71	422.14	773.57	259.24	154.10	38.59%	63.50%
H_2O	390.33	2299.19	3143.67	930.29	866.62	59.54%	62.31%
BeH_2	563.95	1780.19	2285.76	959.14	809.33	58.04%	64.59%
NH_3	452.43	10758.05	17041.33	8340.62	5230.90	22.47%	51.37%

* The "Reduction" results indicate the circuit depth reduction ratios of GBEF and its Ablation relative to ADAPT-ϵ_2, which represents the state-of-the-art algorithm achieving chemical accuracy with the shallowest circuit depth.

Tab. 3 compares the final ansatz circuit depths between GBEF (with ablation) and ADAPT-VQE algorithms with different convergence thresholds. We emphasize

that the Jordan-Wigner encoding [12] is employed here to transform excitations to quantum circuits. While alternative methods could produce shallower circuit, the conclusion still holds. Tab. 3 demonstrates that our GBEF achieves further circuit depth reduction compared to the current best algorithm – ADAPT-ϵ_2, reaching up to about 60% reduction (with ablation studies showing a 65% upper bound). These results confirm that our GBEF method generates circuits that are more executable on NISQ devices and capable of producing meaningful results, owing to their shallower depth.

Tab. 4 summarizes the runtime performance of GBEF versus ADAPT-VQE algorithms for UCCSD ansatz simplification. The data reveal that as molecular size increases, GBEF demonstrates progressively more significant acceleration over ADAPT-ϵ_2. Notably, GBEF achieves a over 600× speedup for NH_3. Benefiting from its lower computational complexity, the GBEF can efficiently handle UCCSD ansatz simplification for large molecular systems.

Table 4: Comparison of runtime between GBEF and ADAPT-VQE algorithms with different convergence thresholds. All ADAPT-VQE implementations are classically simulated due to current quantum hardware limitations.

Molecule	ADAPT-			GBEF	Speedup* (×)
	ϵ_1	ϵ_2	ϵ_3		
H_4	3.05s	5.73s	10.08s	0.45s	12.73
HF	2.66s	8.38s	21.75s	0.91s	9.21
H_2O	26.38s	164.96s	365.59s	1.96s	84.16
BeH_2	42.86s	145.29s	314.67s	1.62s	89.69
NH_3	471.23s	6275.84s	8185.81	9.25s	678.47

* The "Speedup" values indicate the acceleration factor of GBEF relative to ADAPT-ϵ_2, as it represents the best algorithm achieving chemical accuracy with the shallowest circuit depth.

Fig. 2 visually compares the Potential Energy Surfaces (PES), VQE errors compared with FCI results, and parameter distributions obtained by different algorithms for three investigated molecular systems (H_4, H_2O and BeH_2). As visualized in Fig. 2, Hartree-Fock and ADAPT-ϵ_1 fail to meet the chemical accuracy standard, while UCCSD, ADAPT-ϵ_2, ADAPT-ϵ_3, GBEF and its Ablation maintain acceptable errors across all bond lengths. ADAPT-ϵ_3 achieves comparable solution accuracy to UCCSD, but requires substantially more parameters (similar to SymUCCSD). While ADAPT-ϵ_2 currently represents the state-of-the-art method by balancing accuracy and parameter efficiency, our GBEF and Ablation achieve superior parameter reduction. A particularly valuable observation is that within the bond length range of 0.7-1.0 Å for the BeH_2 molecule, both GBEF and ADAPT-ϵ_1 take identical parameters, even though the implementation cost of GBEF is significantly lower than that of ADAPT-ϵ_1.

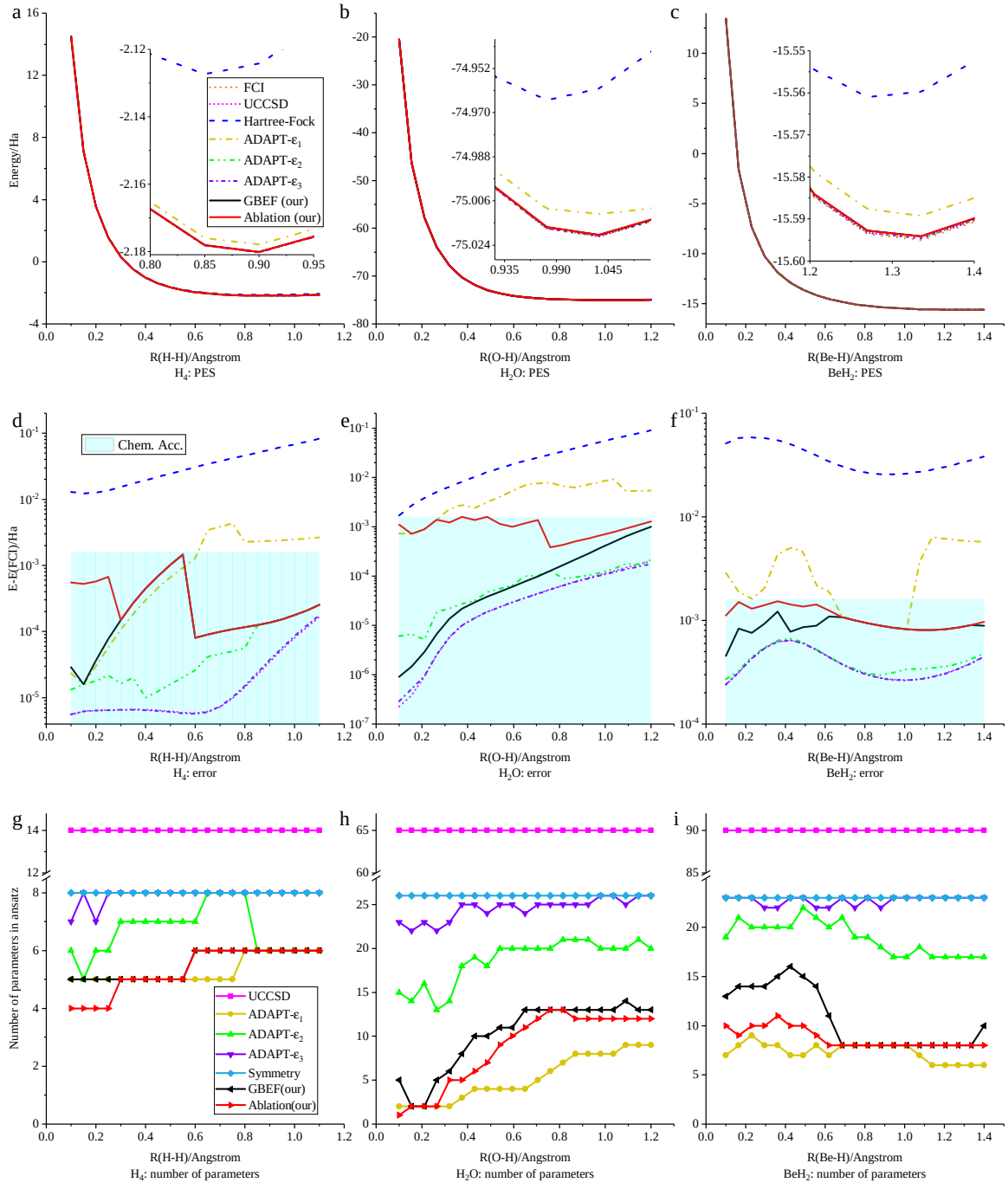

Figure 2: Potential energy surfaces (a-c), solution errors (d-f), and parameter count distributions (g-i) versus bond length obtained by different algorithms for the H_4, H_2O, and BeH_2 molecular systems. Shaded blue region represents area within "Chem. Acc." as 1.6 mHa.

4. Conclusion

This paper presents an efficient method for filtering out non-critical excitations in the UCCSD ansatz, enabling the construction of shallower quantum circuits for molecular ground-state energy calculations. We establish a fundamental connection between the excitations' gradients at Hartree-Fock state and their correlation energy contributions, and propose a gradient-based excitation sorting and truncation protocol. By compressing both the Hamiltonian and Hartree-Fock state into the excitation's subspace, these gradients can be efficiently calculated in parallel on classical computers. Additionally, we propose grouping the excitations based on the involved free parameters and utilizing spin-adaptation constraints to reduce the number of gradient computations. Compared to existing best ADAPT-VQE algorithm, the GBEF algorithm achieves about 20-46% parameter decrease, 15-60% circuit depth reduction, and 9-678× runtime speedup in the investigated molecules while maintaining chemical accuracy, demonstrating significantly improved feasibility for near-term experimental applications.

5. APPENDIX

Theorem 1. *If the Hartree-Fock state $|HF\rangle$ is a good approximation to the exact ground state wave-function $|\Phi_0\rangle$, an excitation's contribution to the correlation energy is related to the gradient of the system energy involved only this excitation at the $|HF\rangle$ with respect to the coefficient $\theta = 0$.*

Proof. We refer to the exact ground state of the system in the single- and double-excitation subspace as $|\Phi_0\rangle$, which can be written as the following form in the configuration interaction expansion:

$$|\Phi_0\rangle = c_0|HF\rangle + \sum_{a,r} c_a^r|\Psi_a^r\rangle + \sum_{a>b,r>s} c_{ab}^{rs}|\Psi_{ab}^{rs}\rangle, \tag{15}$$

where the singly excited determinants $|\Psi_a^r\rangle = A_a^r|HF\rangle$ are obtained by replacing the spin orbital χ_a with χ_r in the $|HF\rangle$, while the doubly excited determinants $|\Psi_{ab}^{rs}\rangle = A_{ab}^{rs}|HF\rangle$ involve simultaneous substitutions of $\chi_a \to \chi_r$ and $\chi_b \to \chi_s$. These determinants obey the orthonormality condition: $\langle\Psi_i|\Psi_j\rangle = \delta_{ij}$.

The system Hamiltonian $\mathscr{H}$ satisfies the eigenrelation with the ground state $|\Phi_0\rangle$:

$$\mathscr{H}|\Phi_0\rangle = \mathscr{E}_0|\Phi_0\rangle, \tag{16}$$

with $\mathscr{E}_0$ referring to the exact ground energy. By substracting the term $E_{HF}|\Phi_0\rangle$ from both sides, the above equation transforms to

$$(\mathscr{H} - E_{HF})|\Phi_0\rangle = (\mathscr{E}_0 - E_{HF})|\Phi_0\rangle = E_{\text{corr}}|\Phi_0\rangle, \tag{17}$$

where E_{HF} denotes the energy of Hartree-Fock state, i.e., $E_{HF} = \langle HF|\mathscr{H}|HF\rangle$, and E_{corr} is the interested electron correlation energy, respectively. If we multiply this

equation by $\langle HF|$, we obtain

$$\langle HF|(\mathscr{H} - E_{HF})|\Phi_0\rangle = E_{\text{corr}}\langle HF|\Phi_0\rangle = c_0 E_{\text{corr}}. \tag{18}$$

After, we expand the term $|\Phi_0\rangle$ on the left-hand side using Eq. (15), yielding

$$\begin{aligned}\langle HF|(\mathscr{H} - E_{HF})|\Phi_0\rangle &= \langle HF|(\mathscr{H} - E_{HF})\left(c_0|HF\rangle + \sum_{a,r} c_a^r|\Psi_a^r\rangle + \sum_{a>b,r>s} c_{ab}^{rs}|\Psi_{ab}^{rs}\rangle\right) \\ &= \sum_{a>b,r>s} c_{ab}^{rs}\langle HF|\mathscr{H}|\Psi_{ab}^{rs}\rangle,\end{aligned} \tag{19}$$

where the Brillouin's theorem ($\langle HF|\mathscr{H}|\Psi_a^r\rangle = \langle\Psi_a^r|\mathscr{H}|HF\rangle = 0$) [4] is imposed. Combining Eqs. (18) and (19), the electron correlation energy E_{corr} emerges as

$$E_{\text{corr}} = \sum_{a>b,r>s} \frac{c_{ab}^{rs}}{c_0}\langle HF|\mathscr{H}|\Psi_{ab}^{rs}\rangle. \tag{20}$$

Thus, the electronic correlation energy fundamentally comprises a weighted summation of interaction terms $\langle HF|\mathscr{H}|\Psi_{ab}^{rs}\rangle$.

For a given excitation $A \in \{\hat{a}_r^\dagger\hat{a}_a - \hat{a}_a^\dagger\hat{a}_r, \hat{a}_r^\dagger\hat{a}_s^\dagger\hat{a}_a\hat{a}_b - \hat{a}_a^\dagger\hat{a}_b^\dagger\hat{a}_r\hat{a}_s\}$, the gradient of system energy (or alternatively denoted as the excitation's gradient, for simplicity) with respect to the excitation's coefficient $\theta = 0$ is

$$\frac{\mathrm{d}E}{\mathrm{d}\theta}\Big|_{\theta=0} := \frac{\mathrm{d}}{\mathrm{d}\theta}\langle HF|\mathrm{e}^{-\theta A}\mathscr{H}\mathrm{e}^{\theta A}|HF\rangle|_{\theta=0} = \langle HF|[\mathscr{H}, A]|HF\rangle. \tag{21}$$

For a double excitation A_{ab}^{rs}, this gradient is

$$\frac{\mathrm{d}E}{\mathrm{d}\theta}\Big|_{\theta=0} = \langle HF|\mathscr{H}|\Psi_{ab}^{rs}\rangle + \text{h.c.}$$

Due to the hermiticity of $\mathscr{H}$, for real determinations $|\Psi_{ab}^{rs}\rangle$ and $|HF\rangle$, $\frac{\mathrm{d}E}{\mathrm{d}\theta}\big|_{\theta=0} = 2\langle HF|\mathscr{H}|\Psi_{ab}^{rs}\rangle$. Combining with Eq. (19), this result implies that the gradient of the excitation in $|HF\rangle$ when its associated parameter $\theta = 0$ is related to its contribution to the electron correlation energy E_{corr}. If the $|HF\rangle$ is a good approximation to the $|\Phi_0\rangle$, its coefficient c_0 will be larger than any of others in the configuration interaction expansion Eq. (15), leading to the weights in Eq. (20) $\left|\frac{c_{ab}^{rs}}{c_0}\right| \leq 1$. If $|\langle HF|\mathscr{H}|\Psi_{ab}^{rs}\rangle| \approx 0$, the corresponding contribution $\frac{c_{ab}^{rs}}{c_0}\langle HF|\mathscr{H}|\Psi_{ab}^{rs}\rangle$ in Eq. (20) becomes negligible. This implies that the gradient of a double excitation when its parameter $\theta = 0$ reflects its contribution to the correlation energy.

Analogously, the gradient of a single excitation A_a^r at $|HF\rangle$ when $\theta = 0$ is $\frac{\mathrm{d}E}{\mathrm{d}\theta}\big|_{\theta=0} = 2\langle HF|\mathscr{H}|\Psi_a^r\rangle = 0$, because of the Brillouin's theorem. This result is consistent with the empirical observation that the inclusion of single excitations often contributes negligibly to ground-state energy calculations. □

In some more refined computational scenarios, the contributions of single excitations have to be taken into account. Although single excited states do not directly interact with the Hartree-Fock state, they indirectly influence the system's energy by modifying the coefficients of double excited states, since $\langle\Psi_a^r|\mathscr{H}|\Psi_{bc}^{st}\rangle \neq 0$ when $a \in \{b, c\}$.

Data and code availability

The code and data used or presented in this paper are openly available on Gitee at `https://gitee.com/mindspore/mindquantum/tree/research/paper_with_code`.

Acknowledgments

The authors thank Junyuan Zhou, Keli Zheng, Dingchao Gao, Riling Li for their valuable discussion. This work is sponsored by Innovation Program for Quantum Science and Technology under Grant No. 2024ZD0300502, Beijing Nova Program Grant No. 20220484128 and 20240484652, and CPS-Yangtze Delta Region Industrial Innovation Center of Quantum and Information Technology-MindSpore Quantum Open Fund.

References

[1] Sam McArdle, Suguru Endo, Alan Aspuru-Guzik, Simon C Benjamin, and Xiao Yuan. Quantum computational chemistry. *Reviews of Modern Physics*, 92(1):015003, 2020.

[2] Henry Eyring. The activated complex in chemical reactions. *The Journal of chemical physics*, 3(2):107–115, 1935.

[3] Trygve Helgaker, Sonia Coriani, Poul Jørgensen, Kasper Kristensen, Jeppe Olsen, and Kenneth Ruud. Recent advances in wave function-based methods of molecular-property calculations. *Chemical reviews*, 112(1):543–631, 2012.

[4] Attila Szabo and Neil S Ostlund. *Modern quantum chemistry: introduction to advanced electronic structure theory*. Courier Corporation, 1996.

[5] Michael A Nielsen and Isaac L Chuang. *Quantum Computation and Quantum Information 10th Anniversary Edition*. Cambridge University Press, 2010.

[6] Daniel S Abrams and Seth Lloyd. Quantum algorithm providing exponential speed increase for finding eigenvalues and eigenvectors. *Physical Review Letters*, 83(24):5162, 1999.

[7] John Preskill. Quantum computing in the nisq era and beyond. *Quantum*, 2:79, 2018.

[8] Google AI Quantum, Collaborators, Frank Arute, Kunal Arya, Ryan Babbush, Dave Bacon, Joseph C Bardin, Rami Barends, Sergio Boixo, Michael Broughton, Bob B Buckley, et al. Hartree-fock on a superconducting qubit quantum computer. *Science*, 369(6507):1084–1089, 2020.

[9] Alberto Peruzzo, Jarrod McClean, Peter Shadbolt, Man-Hong Yung, Xiao-Qi Zhou, Peter J Love, Alan Aspuru-Guzik, and Jeremy L Obrien. A variational eigenvalue solver on a photonic quantum processor. *Nature communications*, 5(1):1–7, 2014.

[10] Stasja Stanisic, Jan Lukas Bosse, Filippo Maria Gambetta, Raul A Santos, Wojciech Mruczkiewicz, Thomas E O'Brien, Eric Ostby, and Ashley Montanaro. Observing ground-state properties of the fermi-hubbard model using a scalable algorithm on a quantum computer. *arXiv preprint arXiv:2112.02025*, 2021.

[11] Matthew P Harrigan, Kevin J Sung, Matthew Neeley, Kevin J Satzinger, Frank Arute, Kunal Arya, Juan Atalaya, Joseph C Bardin, Rami Barends, Sergio Boixo, et al. Quantum approximate optimization of non-planar graph problems on a planar superconducting processor. *Nature Physics*, 17(3):332–336, 2021.

[12] Pascual Jordan and Eugene Paul Wigner. *Über das paulische äquivalenzverbot*. Springer, 1993.

[13] Sergey B Bravyi and Alexei Yu Kitaev. Fermionic quantum computation. *Annals of Physics*, 298(1):210–226, 2002.

[14] Abhinav Kandala, Antonio Mezzacapo, Kristan Temme, Maika Takita, Markus Brink, Jerry M

Chow, and Jay M Gambetta. Hardware-efficient variational quantum eigensolver for small molecules and quantum magnets. *Nature*, 549(7671):242–246, 2017.

[15] Jarrod R McClean, Sergio Boixo, Vadim N Smelyanskiy, Ryan Babbush, and Hartmut Neven. Barren plateaus in quantum neural network training landscapes. *Nature communications*, 9(1):4812, 2018.

[16] Yordan S Yordanov, Vasileios Armaos, Crispin HW Barnes, and David RM Arvidsson-Shukur. Qubit-excitation-based adaptive variational quantum eigensolver. *Communications Physics*, 4(1):228, 2021.

[17] Ho Lun Tang, VO Shkolnikov, George S Barron, Harper R Grimsley, Nicholas J Mayhall, Edwin Barnes, and Sophia E Economou. qubit-adapt-vqe: An adaptive algorithm for constructing hardware-efficient ansätze on a quantum processor. *PRX Quantum*, 2(2):020310, 2021.

[18] Yordan S Yordanov, David RM Arvidsson-Shukur, and Crispin HW Barnes. Efficient quantum circuits for quantum computational chemistry. *Physical Review A*, 102(6):062612, 2020.

[19] Mafalda Ramôa, Panagiotis G Anastasiou, Luis Paulo Santos, Nicholas J Mayhall, Edwin Barnes, and Sophia E Economou. Reducing the resources required by adapt-vqe using coupled exchange operators and improved subroutines. *npj Quantum Information*, 11(1):1–19, 2025.

[20] Zhijie Sun, Xiaopeng Li, Jie Liu, Zhenyu Li, and Jinlong Yang. Circuit-efficient qubit excitation-based variational quantum eigensolver. *Journal of Chemical Theory and Computation*, 2025.

[21] Changsu Cao, Jiaqi Hu, Wengang Zhang, Xusheng Xu, Dechin Chen, Fan Yu, Jun Li, Han-Shi Hu, Dingshun Lv, and Man-Hong Yung. Progress toward larger molecular simulation on a quantum computer: Simulating a system with up to 28 qubits accelerated by point-group symmetry. *Physical Review A*, 105(6):062452, 2022.

[22] Harper R Grimsley, Sophia E Economou, Edwin Barnes, and Nicholas J Mayhall. An adaptive variational algorithm for exact molecular simulations on a quantum computer. *Nature communications*, 10(1):3007, 2019.

[23] Luke W Bertels, Harper R Grimsley, Sophia E Economou, Edwin Barnes, and Nicholas J Mayhall. Symmetry breaking slows convergence of the adapt variational quantum eigensolver. *Journal of Chemical Theory and Computation*, 18(11):6656–6669, 2022.

[24] Jules Tilly, Hongxiang Chen, Shuxiang Cao, Dario Picozzi, Kanav Setia, Ying Li, Edward Grant, Leonard Wossnig, Ivan Rungger, George H Booth, et al. The variational quantum eigensolver: a review of methods and best practices. *Physics Reports*, 986:1–128, 2022.

[25] Marco Cerezo, Andrew Arrasmith, Ryan Babbush, Simon C Benjamin, Suguru Endo, Keisuke Fujii, Jarrod R McClean, Kosuke Mitarai, Xiao Yuan, Lukasz Cincio, et al. Variational quantum algorithms. *Nature Reviews Physics*, 3(9):625–644, 2021.

[26] Christian W Bauer, Zohreh Davoudi, Natalie Klco, and Martin J Savage. Quantum simulation of fundamental particles and forces. *Nature Reviews Physics*, 5(7):420–432, 2023.

[27] Vlad O Shkolnikov, Nicholas J Mayhall, Sophia E Economou, and Edwin Barnes. Avoiding symmetry roadblocks and minimizing the measurement overhead of adaptive variational quantum eigensolvers. *Quantum*, 7:1040, 2023.

[28] Naomichi Hatano and Masuo Suzuki. Finding exponential product formulas of higher orders. In *Quantum annealing and other optimization methods*, pages 37–68. Springer, 2005.

[29] Andrew Tranter, Sarah Sofia, Jake Seeley, Michael Kaicher, Jarrod McClean, Ryan Babbush, Peter V Coveney, Florian Mintert, Frank Wilhelm, and Peter J Love. The b ravyi–k itaev transformation: Properties and applications. *International Journal of Quantum Chemistry*, 115(19):1431–1441, 2015.

[30] Shashank G Mehendale, Bo Peng, Niranjan Govind, and Yuri Alexeev. Exploring parameter redundancy in the unitary coupled-cluster ansatze for hybrid variational quantum computing. *The Journal of Physical Chemistry A*, 127(20):4526–4537, 2023.

[31] Trygve Helgaker, Poul Jorgensen, and Jeppe Olsen. *Molecular electronic-structure theory*. John Wiley & Sons, 2013.

[32] Jarrod R McClean, Nicholas C Rubin, Kevin J Sung, Ian D Kivlichan, Xavier Bonet-Monroig,

Yudong Cao, Chengyu Dai, E Schuyler Fried, Craig Gidney, Brendan Gimby, et al. Openfermion: the electronic structure package for quantum computers. *Quantum Science and Technology*, 5(3):034014, 2020.

[33] Xusheng Xu, Jiangyu Cui, Zidong Cui, Runhong He, Qingyu Li, Xiaowei Li, Yanling Lin, Jiale Liu, Wuxin Liu, Jiale Lu, Maolin Luo, Chufan Lyu, Shijie Pan, Mosharev Pavel, Runqiu Shu, Jialiang Tang, Ruoqian Xu, Shu Xu, Kang Yang, Fan Yu, Qingguo Zeng, Haiying Zhao, Qiang Zheng, Junyuan Zhou, Xu Zhou, Yikang Zhu, Zuoheng Zou, Abolfazl Bayat, Xi Cao, Wei Cui, Zhendong Li, Guilu Long, Zhaofeng Su, Xiaoting Wang, Zizhu Wang, Shijie Wei, Re-Bing Wu, Pan Zhang, and Man-Hong Yung. Mindspore quantum: A user-friendly, high-performance, and ai-compatible quantum computing framework, 2024.

[34] Charles G Broyden. Quasi-newton methods and their application to function minimisation. *Mathematics of Computation*, 21(99):368–381, 1967.

Author contributions

RH He, and SG Ying established the key idea in this paper. RH He and QZ Chai did the numerical experiments. RH He, QZ Chai and X Hong wrote the first version of the draft paper. All the authors contributed to the preparation of this paper.

Competing interests

The authors declare no competing interests.

Correspondence

Correspondence and requests for materials should be addressed to RH He or SG Ying.